Technical Paper

ISSN 1997-1400 Int. J. Pavement Res. Technol. 5(2):108-114
Copyright @ Chinese Society of Pavement Engineering

Substrate Restraints of Bonded Concrete Overlays

Alex Hak-Chul Shin[1+], and David A. Lange[2]

Abstract: The performance of bonded concrete overlays can be reduced by early age surface cracking and/or debonding at the interface between old and new concrete. These early age failures are mainly due to volume changes of the overlay concrete by shrinkage, thermal changes, and substrate restraints. In the analysis and design of bonded concrete overlays, the substrate restraint is often disregarded. This study illustrates how the substrate restraint affects the surface stress and contributes to early age surface cracking of bonded concrete overlays by comparing three restraint conditions. Practical insights on how to minimize cracking due to shrinkage, thermal changes, and substrate restraints are provided. One conclusion from this study is that an improved analysis can be achieved if the Westergaard-Bradbury solution is modified to include internal stress from horizontal restriction in bonded concrete overlays.

***Key words**: Bonded concrete overlay; Drying shrinkage; Early age behavior; Surface cracking.*

Introduction

Bonded concrete overlays are often a cost-effective alternative for the rehabilitation of concrete pavements through the increase of pavement thickness. Bonded concrete overlays use the old concrete pavement as a substrate, and new overlay concrete is added to the top. This strategy minimizes construction time and costs and can maintain overhead clearance compared to unbonded overlays. Due to joints and cracks of the substrate, however, a thin overlay is vulnerable to reflection cracking.

Concrete undergoes volume change due to changes in environmental conditions, such as temperature and humidity. Volume changes in new concrete can lead to cracking during the first few days after concrete placement. The major sources of volume changes include drying shrinkage and thermal contraction. The volume changes can create high stresses at the surface of the new overlay concrete and/or at the interface between the concrete layers.

While the new overlay concrete is affected by drying shrinkage and temperature changes, the old substrate concrete is relatively stable. When new concrete is placed upon old concrete pavement as a bonded overlay, the old concrete substrate acts as a restraint to any volume change caused by shrinkage and thermal changes in the new concrete. Analysis of the residual stresses in bonded concrete overlay requires consideration of the restraint imposed by the old concrete substrate.

In this study, analytical solutions and numerical analyses were performed to investigate the substrate restraint of bonded concrete overlays subjected to shrinkage and thermal changes. This study develops a model that shows the increase of tensile stress at the top surface at night, which is considered a vulnerable time for surface cracking at an early pavement age. This research leads to suggestions in construction practice to minimize early age failure of bonded concrete overlays due to surface cracking.

Analytical Solutions of Bonded Concrete Overlays

This study focuses on early age surface cracking, and a case study was used as an example for the analysis. The analytical solution will be presented, addressing our application of a classical elasticity solution to the case of non-linear gradients of temperature and shrinkage.

Elasticity Solution

For a thin, finite slab subjected to non-linear temperature gradient, as shown in Fig. 1, the thermal stress for no restraint condition is expressed as follows [1]:

$$\sigma_x = \sigma_z = -\frac{\alpha \Delta T(y) E_c}{1-\nu} + \frac{1}{2c(1-\nu)}\int_{-c}^{c} \alpha \Delta T(y) E_c\, dy - \frac{3y}{2c^3(1-\nu)}\int_{-c}^{c} \alpha \Delta T(y) E_c\, y\, dy \tag{1}$$

where:
σ_x and σ_z = stress in x- and z-direction,
α = thermal expansion coefficient,
$\Delta T(y)$ = thermal gradient through the thickness of the slab,
E_c = elastic modulus of concrete,
ν = Poisson's ratio, and
y = distance from the slab centroid.

In Eq. (1), the second term is related to axial restraints, and the third term is related to curvature restraints. Therefore, if axial and/or curvature restraints are imposed, the corresponding terms would cancel out. For the case where axial expansion is free and curvature is restrained, the thermal stress will follow Eq. (2):

$$\sigma_x = \sigma_z = -\frac{\alpha \Delta T(y) E_c}{1-\nu} + \frac{1}{2c(1-\nu)}\int_{-c}^{c} \alpha \Delta T(y) E_c\, dy \tag{2}$$

[1] Department of Civil and Environmental Engineering, Louisiana State University, 3505-C Patrick Taylor Hall, Baton Rouge, LA 70803, USA.
[2] Department of Civil and Environmental Engineering, University of Illinois at Urbana-Champaign, 205 N. Mathews, MC-205, Urbana, IL 61801, USA.
[+] Corresponding Author: E-mail shin@lsu.edu
Note: Submitted July 1, 2011; Revised September 20, 2011; Accepted October 5, 2011.

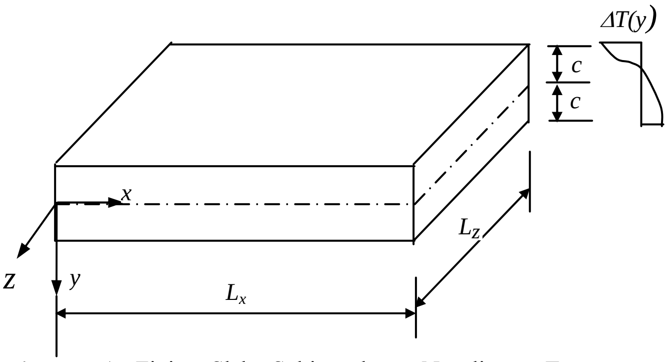

Fig. 1. A Finite Slab Subjected to Non-linear Temperature Gradients.

The calculated thermal stress is identical to the Westergaard solution [2] if the base plate is relatively stiff (i.e., modulus of subgrade reaction is high). Compared to the Westergaard solution, Eq. 2 is useful for nonlinear temperature gradients. Also, Eq. 2 can be modified to calculate the thermal stress of bonded overlays. Since a bonded overlay is restrained by a substrate slab in axial and curvature manner, the axial restraint's term in Eq. (2) should be cancelled out, resulting in the following:

$$\sigma_x = \sigma_z = -\frac{\alpha \Delta T(y) E_c}{1-v} \tag{3}$$

Westergaard-Bradbury Solution

The Westergaard-Bradbury equation [2, 3] is frequently used to calculate stresses in pavement due to linear temperature changes. The equation is based on the elasticity and assumed reaction stress proportional to the deflection of the foundation. For a finite slab with lengths L_x in the x direction and L_z in the z direction (Fig. 1), stresses in the x and z directions can be expressed as follows:

$$\sigma_x = \frac{\alpha \Delta T(y) E_c}{2(1-v^2)}(C_x + vC_z) \tag{4}$$

$$\sigma_x = \frac{\alpha \Delta T(y) E_c}{2(1-v^2)}(C_z + vC_x) \tag{5}$$

Where:
α = thermal expansion coefficient,
E_c = elastic modulus of concrete,
v = Poisson's ratio, and
C_x and C_z = correction factions.
The correction factors C_x and C_z respectively depend on L_x/l and L_z/l, where l is the radius of relative stiffness defined as follows:

$$\iota = \left[\frac{E(2c)^3}{12(1-v^2)k}\right]^{1/4} \tag{6}$$

in which $2c$ is the thickness of the slab and k is the modulus of subgrade reaction. Bradbury developed a simple chart to determine the correction factors based on the Westergaard solution.

According to Mohamad's formulation [4], a slab subjected to a non-linear temperature gradient can be analyzed by dividing thermal stresses into residual and curvature stresses. Residual stresses develop from internal restraint to satisfy the equilibrium of the slab. The residual stress equation is as follows:

$$\sigma_{res} = \frac{\alpha E_c}{(1-v)\left[-\Delta T(y) + \frac{1}{2c}N^* - \frac{3y}{2c^3}M^*\right]} \tag{7}$$

$$N^* = \int_{-c}^{c} \Delta T(y) dy \tag{8}$$

$$N^* = \int_{-c}^{c} \Delta T(y) y dy \tag{9}$$

Constants represent the same values as the previous equations.

An equivalent curvature for the slab is as follows:

$$k = -\frac{12\alpha M^*}{(2c)^3} = -\frac{3\alpha M^*}{2c^3} \tag{10}$$

An equivalent linear temperature gradient that produces the same curvature as the Westergaard solution is calculated using the following equation:

$$\Delta T_{eqv} = -\frac{2ck}{\alpha} \tag{11}$$

The Westergaard-Bradbury equation is used to calculate curvature stresses for the equivalent linear temperature gradient. Total stress is the summation of residual and curvature stresses.

A Case Study: Surface Cracking at Willard Airport

This project on bonded concrete overlays was motivated by trial sections constructed on a runway of the Champaign Willard Airport. The trial section consisted of 8-in thick, normal concrete pavement placed upon the existing concrete pavement. The existing pavement consisted of 10-in thick concrete pavement with transverse joints of 15-ft spacing with no dowel bars. The mixture design of the existing concrete is not known, but the aggregate is made of crushed limestone. The trial section was considered a bonded overlay because new concrete was cast directly on existing concrete, and no bond-breaker layer was used.

The trial section of concrete bonded overlay was placed on the runway section during the morning of July 21, 1998. The next morning, cracks were observed in the overlay at approximately 4-ft spacing in the transverse direction. The transverse joints were placed at 15-ft spacing with no dowel bars. The concrete mix design and construction details can be found in an Illinois Department of Transportation (IDOT) report [5].

The temperature of the fresh concrete was measured at the time of placement to be 89°F. The ambient temperature during placement was in the mid-80°s, and the temperature rose to 95°F in the afternoon. The temperature dropped from 90°F between 7:00 P.M. and midnight. At around 5:00 A.M., there was rain, and the temperature dropped to 71°F. The cracks were first observed at

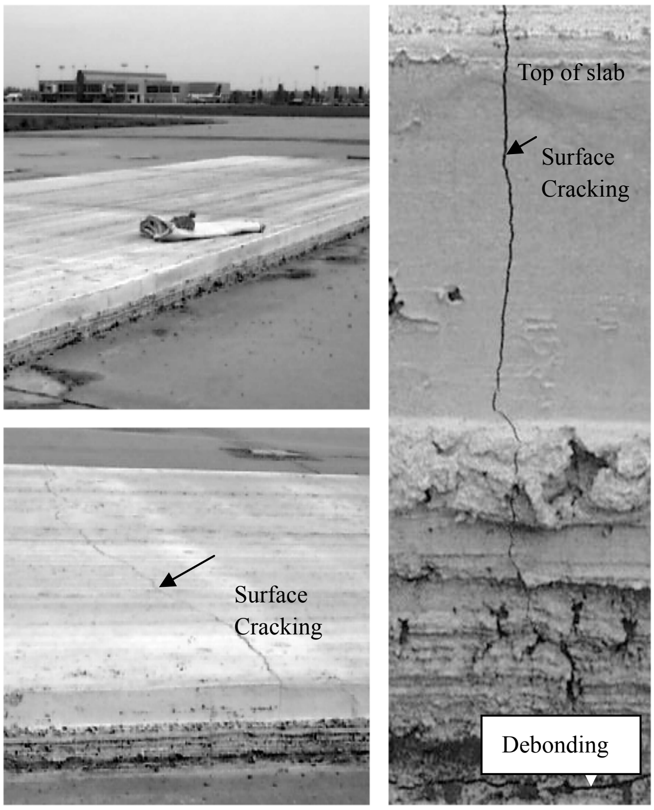

Fig. 2. Surface Cracks Developed in the Runway at Willard Airport.

approximately 8:00 A.M. on July 22, 1998. Photographs taken at Willard Airport are shown in Fig. 2. The photograph in the top left shows a general view of the bonded overlay trial slab. Cracks extended across the slab, as shown in the picture at the lower left. A crack opened at the top and was restrained at the interface with some interfacial debonding (picture on the right).

This case study was part of an investigation to understand the stress distribution due to shrinkage and thermal changes that lead to cracking. The effect of substrate restraint was specifically investigated by using analytical solutions available in literature.

Material Properties

IDOT C1 Mix

The overlay concrete used on the runway section at Willard Airport was IDOT C1 mix. This C1 mix has a low water-to-cementitious material (w/cm) ratio of 0.42 combined with a high proportion of Class C fly ash. For the laboratory experiments, available laboratory materials were used instead of in-situ constituents. The laboratory materials were similar to the field materials with the exception of Portland cement. While Type III cement was used for the field trial overlay, Type I Portland cement with limestone aggregate and natural sand was used in the concrete mixture design in the laboratory test. Types I and III have a similar chemical composition, but Type III delivers higher fineness results in early strength development. Using different types of cement may largely affect the development strength and elastic modulus but cause a minor effect on shrinkage and thermal changes. The measured elastic modulus and compressive strength were used for the analysis later.

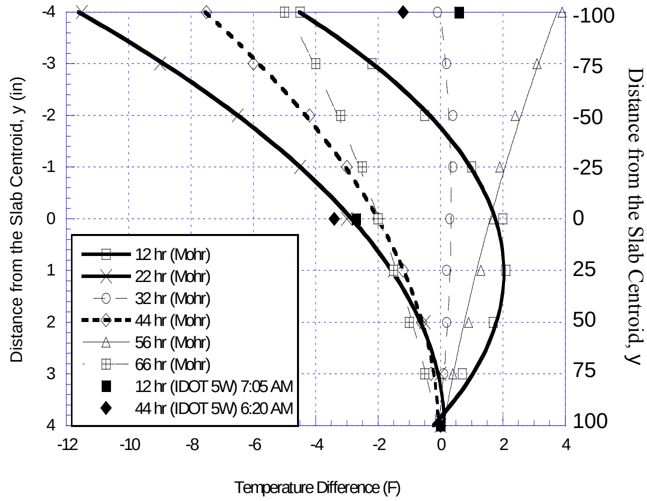

Fig. 3. Temperature Gradient within Overlay during the First 66 Hours after Placement.

Thermal Gradient in Overlay Due to the Heat of Hydration

The temperature gradient through the overlay thickness was investigated using the literature and test data available from the field trial. Using an existing model by Mohr et al. that predicts temperature gradients through the thickness of concrete overlays at an early age [6], the model assumes concrete properties and environmental conditions that are not largely different from those experienced during the field trial. The model predictions, shown in Fig. 3, illustrate how the temperature gradient changes within the first two days after the overlay is placed. The figure designates the temperature at the overlay-substrate interface as a zero point. The largest tensile stress occurs at about 22 hours after the placement of new concrete on old concrete due to a temperature gradient of about 12°F between the top of the overlay and the bottom of the overlay. For reference, temperatures measured at Lane 5W in the Willard test section are presented in Fig. 3. The measured temperatures in the middle of the overlay slab ($y = 0$) are close to Mohr's data, while the temperatures at the top surface (y = -4 in) are much lower than Mohr's data. Interestingly, the Lane 5W in the Willard test section did not crack [5, 7].

Drying Shrinkage

The shrinkage gradient of concrete was calculated from the measured shrinkage and pore relative humidity (RH) in the concrete, as explained in detail in Shin's dissertation [8]. Two companion specimens with dimensions of 3×3×40 in (76.2×76.2×1,016 mm) were used to measure creep and shrinkage strains. One of the specimens was allowed free movement while the other specimen was restrained through the application of the necessary external load to keep the length constant. Shrinkage strains were measured in the free shrinkage specimen. Elastic strains measured in the restrained specimen were used to calculate creep strain and other mechanical properties such as shrinkage stresses and creep coefficient. Relative humidity of internal material was measured using five PVC tubes installed in a 3-in concrete block at various depths from the surface

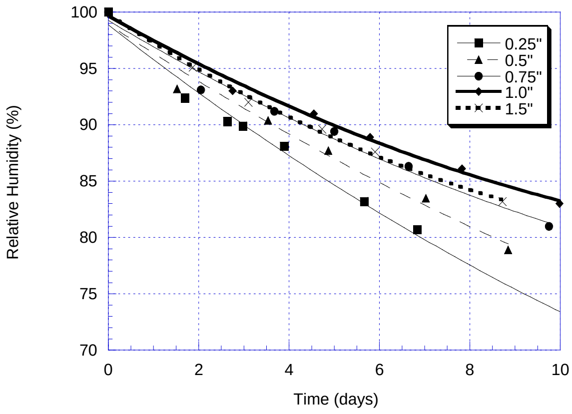

Fig. 4. Measured Pore RH and Fitted 2nd Order Polynomial Curve of Mix C1 Concrete from the IDOT Project.

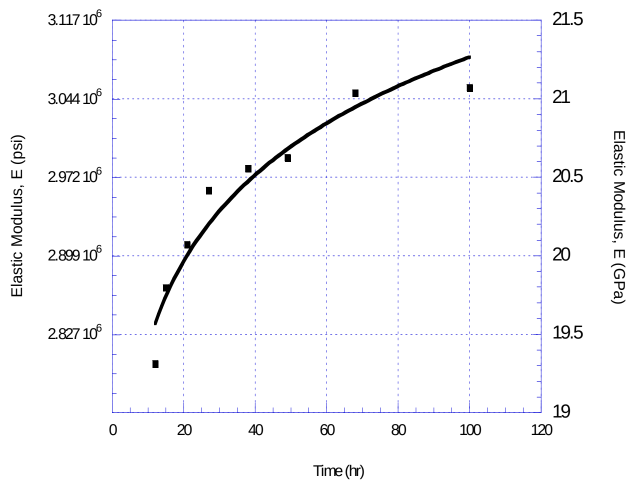

Fig. 5. Evolution of the Elastic Modulus of Overlay Concrete.

(0.25-in, 0.5-in, 0.75-in, 1.0-in, and 1.5-in). The RH profile was used to characterize the shrinkage stress gradient. A calibrated humidity gauge with a probe (Omega gauge) was used to measure pore RH in a tube one at a time. The tube was sealed with cork caps except during the measurement. Fig. 4 shows the measured pore RH at five different depths in the 3-in concrete block. The measured pore RH shows that the pore RH at the depth of 1.5 in was lower than at the depth of 1.0 in. It is reasonable to assume that the pore RH is constant deeper than 1.0 in. The measured moisture profile in an 8-in PCC pavement rapidly changes in the top 1.5 in, but the change is very small in deeper locations [9]. This observation shows that the pore RH profile of a 3-in concrete block can be used in an 8-in overlay.

From the measured pore RH, 2nd order polynomial equations that best fit each depth of overlay concrete were obtained. Using these polynomial equations, pore RH at distinct time intervals can be calculated. In addition, creep-shrinkage tests were performed to measure the gross shrinkage and creep of the IDOT C1 mix. Drying shrinkage gradients and creep gradients of the 8-in overlay was constructed as detailed in Shin's dissertation [8] and used for the numerical analysis.

To simultaneously consider both drying shrinkage and temperature as the source of surface cracking behavior, an equivalent temperature was introduced. The equivalent temperature is the summation of a measured temperature and the shrinkage equivalent temperature. The use of equivalent temperature is limited by material models in *ABAQUS* [10]. *ABAQUS* does not provide a provision for modeling drying shrinkage, but this problem was overcome by the use of an equivalent temperature.

Elastic Modulus

The elastic modulus of the overlay concrete (IDOT C1 mix) was directly measured by physical tests. Fig. 5 shows the development of the elastic modulus (E) of IDOT C1 mix. The value of elastic modulus was measured soon after the set. The earliest measurement at 12 hours after placement showed that E=2.8x106 psi (=19.2 GPa) and a modest rise thereafter to 3.0x106 psi (=20.7 GPa). A constant value of 3.0×10^6 psi is used in the numerical analysis described in this study.

Three Different Solutions

Two different analytical solutions presented in earlier sections are used to calculate stresses in the slab subject to temperature gradients and different boundary conditions at the bottom of the slab. In addition to those solutions, a numerical solution using a finite element method (FEM) software, *ABAQUS*, is presented for comparison and further application.

The two-dimensional FEM model uses eight-node plane strain elements (CPE8) for overlay and substrate. The aspect ratio of the element was kept at less than 2.0. The interface between two layers was modeled with "contact pair." The bottom surface of the overlay and the top surface of the substrate are a contact pair with small sliding allowed. The contact pair remains in a bonded state if the fracture criterion is less than 1.0 within the given tolerance of 0.05. The dimension of the model is identical to the trial section at Willard Airport. The measured material properties of overlay concrete were used. For old substrate concrete, typical material properties were used.

Poisson's ratio of the overlay material and substrate concrete was assumed to be constant (ν = 0.19). The thermal expansion coefficient was assumed to be constant with time. The same value of $\alpha = 10\times10^{-6}/°C = 5.6\times10^{-6}/°F$ was used for the overlay and substrate materials. The unit weight of the overlay concrete was also considered to be constant with $\gamma = 2.3\times10^{-6}$ kg/mm^3 = 143 lb/ft^3. More details of the FEM model can be found in Shin's dissertation [8].

Role of Substrate Restraints on Stress Distribution

The role of restraint in bonded overlays can be defined using the elastic solution [1]. Fig. 6 compares the state of thermally induced stress (at 22 hours after placement) through the thickness of an 8-in overlay for three different restraint conditions. Case 1 (no restraint) represents the internal stress induced by the 22 hours of thermal gradient (refer to Fig. 3) for a hypothetical "floating" slab without vertical or horizontal restraints. Case 2 restricts curvature deformation but allows horizontal contraction. Case 3 restrains both

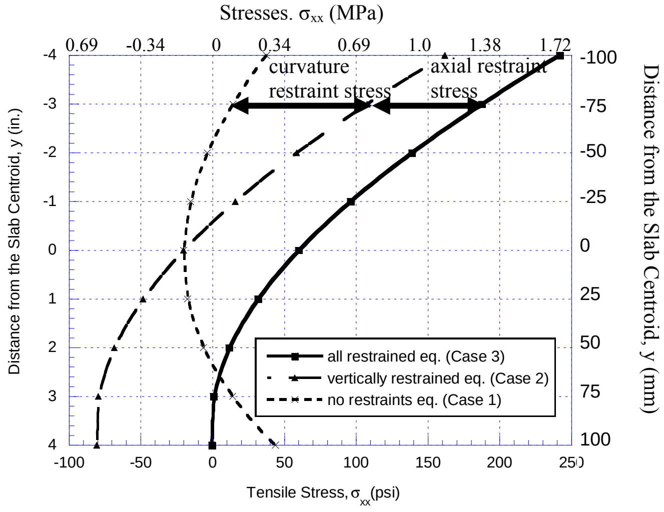

Fig. 6. Stress Distribution through Overlay Thickness for Three Restraint Conditions at 22 Hours after Casting.

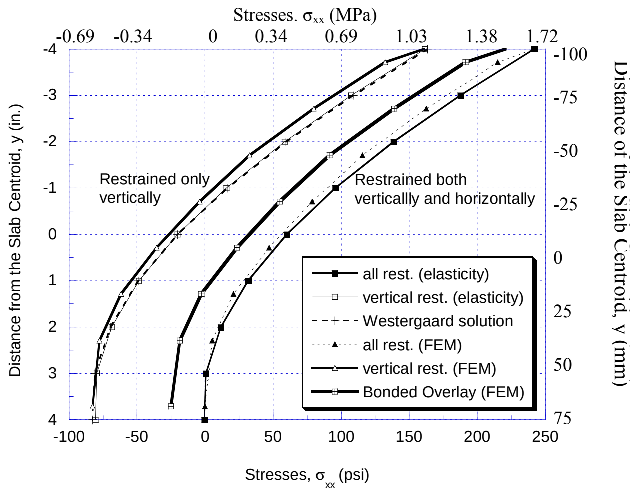

Fig. 7. Comparison of Three Different Solutions for Three Different Restraint Conditions.

curling and horizontal contraction similar to bonded overlays. Thus, one can see that the restraint conditions play a clear role in defining the distribution of internal stress and the bonded condition (Case 3) exhibits the greatest tensile stress at the top surface (i.e., 250 psi = 1.72 MPa for the assumed thermal gradient).

Comparison of Three Different Solutions

To compare the stresses calculated from the three different solutions, the thermal gradient used in the previous section was selected. Two restraint conditions, a vertical-only restraint (Case 2) and a vertical-horizontal restraint (Case 3), were considered in this study. Fig. 7 shows the calculated stresses through the depth of the overlay. For the vertically restrained condition, the three different solutions predict nearly the same stress levels throughout the overlay depth. Since the Westergaard solution is limited to the vertically restrained condition, only the elastic solution and FEM solution were considered for the condition restrained both vertically and horizontally. Again, the two solutions produced similar results.

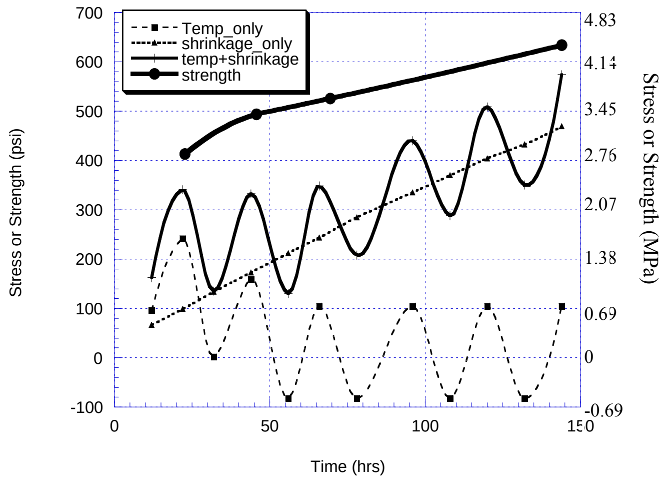

Fig. 8. Tensile Stress at the Top Surface of Bonded Overlay Due to Thermal and Shrinkage Gradients.

One noteworthy result is seen in the FEM solution for bonded overlay. In this solution, the substrate concrete was modeled with finite element, and typical material properties were used. As expected, the actual stress state of the bonded overlay is intermediate between the two restrained conditions analyzed before. This observation suggests that neither the elastic solution nor the Westergaard solution predicts the stresses in a bonded overlay where the substrate acts as an elastic restraint. Therefore, the analysis of a bonded overlay may require the use of elastic restraints to produce a more accurate solution.

Crack Tendency in Bonded Overlay at Early Ages

An FEM analysis was conducted to compute the maximum tensile stress at the top surface of the bonded overlay concrete. The model computes stress resulting from both thermal and shrinkage mechanisms. The model uses typical summer temperature history and assumes that the overlay is cast at about 10:00 A.M. Previous research shows that the threat of thermal cracking is most pronounced for overlays cast in the morning hours [6]. If the concrete is cast in the afternoon (or even better, at night), the synchronization of evolved heat with ambient temperatures is more favorable.

Fig. 8 shows the results of this analysis with four curves. The top curve represents the magnitude of concrete strength measured at the construction site during the first 150 hours. The dotted curves represent the separate thermal and shrinkage components of the maximum stress that occurs at the top surface of the overlay. The solid, oscillating curve is the sum of the two components, or the total stress at the top of the overlay. In this analysis, the substrate temperature was assumed to not factor in surface cracking. Once the overlay is placed, the temperature gradient in the substrate can be very small compared to the overlay concrete. The temperature and stress change due to varying substrate temperatures should be further studied and incorporated.

After 22 hours of casting, the total stress curve rises — largely due to thermal contraction — to a value of 340 psi (2.34 MPa). At 22 hours, the predicted tensile strength of the overlay concrete is about 400 psi (2.76 MPa). This indicates high vulnerability to tensile cracking at about 22 hours after casting. In the next 100 hours, the threat of thermal contraction subsides, but the significance of shrinkage stresses may increase. The shrinkage stress depicted in Fig. 8 arises from a non-linear moisture gradient where the top surface at 144 hours is about 80% RH and the bottom of the overlay is at 93% RH. At 144 hours of casting, the total stress curve approaches the strength curve. The value of tensile stress at 144 hours is 580 psi (4.0 MPa) whereas the strength is about 620 psi (4.27 MPa).

Thermal gradient used in the analysis was the combination of thermal and drying shrinkage. The variation of temperature and drying shrinkage was used in time step analysis. In the Fig. 8, it is possible that thermal cracking can occur first, and in the case, stress can be relaxed and the analysis should be different. In our analysis, the stress due to temperature gradient is still less than the developed strength as seen in Fig. 8, and the analysis was continued without stress relaxation. If the shrinkage cracking occurred prior to the stress accumulation, the stress relaxation should be considered also. And this was not considered in this study.

Comparison and Implications

The main finding of the analyses is that thermal contraction is indeed a likely cause for cracking within the first 24 hours. However, thermal gradients gradually decrease and become less significant after 24 hours. Still, the threat of cracking under shrinkage stress may remain significant even after the initial 24-hour threat of thermally induced stress subsides.

Insight for Construction Practice

Mixture Design

To construct a durable bonded overlay, it is necessary to verify that the overlay concrete can resist cracking during the applied loads of its service life, surface cracks at the top of the overlay, and early age debonding at the interface's corner. This research focuses on early age cracks due to shrinkage and thermal changes, so it is reasonable to discuss the effect of mix design on the early age behavior of bonded overlay.

A primary consideration is the role of water-to-cement (w/c) ratio. The w/c ratio of the mix has an impact not only on the shrinkage but also on the bond strength at the interface. There is a trend of shrinkage and creep for each mix with respect to the w/c ratio. The trend implies that shrinkage and creep are related to the w/c ratio. This is a well-known fact in several shrinkage models [11-13].

Strength, workability, and durability are also quite dependent on the w/c ratio. It is reasonable to choose a moderate value of w/c ratio to satisfy all the conditions. To evaluate the role of w/c on debonding and surface cracking, it is recommended to use an analytical tool [14] to choose a safe region for conditions such as span length, climatic data, and thickness of the overlay.

Cement is an important parameter to consider in overlay mix design. It affects the shrinkage and heat of hydration of cement paste. Type IV or II cement is usually used to minimize the heat of hydration in mass concrete and summer construction. Type IV or II cement is slow to gain strength at the early age but later has a higher compressive strength than Type I cement [15]. Also, the adiabatic temperature rise in mass concrete using Type IV or II cement is lower than with other types of cement. These two properties of Type IV or II cement (lower strength at early age and low adiabatic temperature rise) are favorable in bonded overlay construction since the cement provides low stress development through a low elastic modulus and low temperature gradients.

Types I and III have similar chemical compositions but a different fineness. The difference in cement type may largely affect the development of the strength and elastic modulus but only offer a minor effect on shrinkage and temperature. It is advisable to monitor increases in temperature when a different type of cement is used.

The use of SCMs, such as fly ash and slag, can enhance concrete engineering properties as well as contribute sustainability. An addition of fly ash or slag reduces the heat generation during the hydration process, and potential thermal cracking is also mitigated accordingly [16]. The use of fly ash and slag generally decreases the early age strength but increases the long-term strength. When slag was added to the mixture, the strength increased after 7 days while strength development did not occur until 28 days later (when fly ash was added) [17].

Volume and the hardness of the aggregate affect the shrinkage of concrete extensively, as explained by Shin [8]. Unless justified by overriding considerations, lightweight aggregate is not recommended for use in bonded overlays, because it may drive higher than normal shrinkage and result in a higher tendency for surface cracking and interface debonding.

Water reducing admixtures, or superplasticizers, are often used to produce high performance concrete with a low w/c ratio. The admixtures are useful in making durable concrete with better freeze-thaw resistance and high strength. However, caution is needed to prevent high autogeneous shrinkage at early age.

The use of silica fume in high performance concrete (HPC) reduces the pore size of the concrete and hence increases durability. This merit, however, comes with the disadvantage of lower bleeding rates. Due to the low bleeding rates of HPC at an early age, moisture loss from the surface due to evaporation cannot be readily replaced and may contribute to early surface cracking. Therefore, precautions should be taken to supply moisture at the surface through wet curing or evaporation-retarding agents.

Curing

To minimize debonding and surface cracking in bonded overlay, it is necessary to minimize the shrinkage and temperature gradients of overlay concrete. This can be achieved by minimizing the moisture and temperature change. One of the easiest ways is to cover the overlay concrete with plastic sheets and use a curing membrane.

Moisture curing is used as active moisture control in concrete surface after finishing the surface. Ponding, spraying, and sprinkling are commonly used for this purpose.

It is well known that the threat of thermal cracking is most pronounced for overlays cast in the morning hours [6]. The reason for thermal cracking lies behind the synchronization of the concrete temperature's peak with the afternoon's high temperature. Therefore, a suggestion is to alter the construction time so that the peak temperature of overlay concrete occurs at night times, and the weather compensates by being cool.

Summary and Conclusions

This study investigates the role of substrate restraint on the cracking tendency in bonded concrete overlay. An existing model was used to predict the temperature gradients through the thickness of the overlay at an early age. A creep-shrinkage test was performed to measure the shrinkage and creep strains of the IDOT C1 mix used for construction at Willard Airport. Measured drying shrinkage, creep, and RH gradient were used to calculate the shrinkage and creep gradients of the mix. Elastic modulus was also obtained from the creep-shrinkage test. Tensile strength measured at the site was used for comparison with the calculated tensile stress at the top surface of the overlay.

Three different methods were used to calculate stresses inside the overlay concrete, which was subjected to shrinkage and thermal changes. A Westergaard-Bradbury solution modified by Hansen to accommodate non-linear temperature gradient was used with an elastic solution method. A numerical solution using ABAQUS was also presented for the comparison.

To study the role of restraint on stress distribution, the elastic solution was applied in a step-wise fashion to account for temperature change over time. The study shows that the restrained conditions play an important role in determining the distribution of internal stress. The stresses calculated using three different solution methods were compared. For vertically (curvature) restrained conditions, the three methods yielded almost identical results. For vertically and horizontally restrained conditions, the elasticity solution and FEM solution resulted in almost the same stress distribution. The Westergaard-Bradbury solution does not calculate stress distribution for that condition. In a real bonded concrete overlay with a substrate modeled with finite element mesh, the stress states are intermediate between the two conditions, vertically restrained condition and vertically and horizontally restrained condition. Therefore, this study concludes that neither the elastic solution nor the Westergaard-Bradbury solution effectively predicts stress in a bonded overlay when the substrate acts as an elastic restraint. An improved analysis can be achieved when the Westergaard-Bradbury solution is modified to include internal stress due to horizontal restriction in bonded concrete overlays.

A numerical analysis was conducted to compute the maximum stress at the top surface of the bonded overlay, which is subject to shrinkage and thermal changes. From this analysis, the thermal contraction is indeed a likely cause for cracking within the first 24 hours, but the thermal gradients gradually decrease and become less significant thereafter. However, the threat of cracking by shrinkage remains significant even after the initial 24-hour threat of thermally induced stress subsides.

Acknowledgement

The authors acknowledge support from the Federal Aviation Administration Center of Excellence at the University of Illinois and the National Science Foundation (Career Award CMS 96-23467).

References

1. Timoshenko, S.P. and Goodier, J.N. (1982). *Theory of Elasticity*, 3rd Edition, McGraw-Hill Book Company, Singapore.
2. Westergaard, H.M. (1926). Analysis of Stresses in Concrete Pavement Due to Variation of Temperature, *Proceedings of Highway Research Board*, Vol. 6, National Research Council, pp. 201-215, Washington, DC, USA.
3. Bradbury, R.D. (1947). *Reinforced Concrete Pavements*, Wire Reinforcement Institute, Washington DC, USA.
4. Mohamad, A.R. and Hansen, W. (1996). Prediction of Stresses in Concrete Pavements Subjected to Non-linear Gradients, *Cement and Concrete Composites*, 19, pp. 381-387.
5. Lange, D., Rau, N., Bicer, B., and Shin, H.C. (2000). Early Age Behavior of Bonded Concrete Overlays (Report submitted to Illinois DOT).
6. Mohr, P., Hansen, W., and Mohamed, A.R. (1997). Thermal Stresses in Concrete Pavements at Early Ages, *Proceeding of the International Conference on Engineering Materials*, pp. 499-514, Ottawa, Canada.
7. Illinois DOT (1998). *Manual on the Rehabilitation of Runway 14R/32L at Willard Airport,* Springfield, IL, USA.
8. Shin, H.C. (2000). Early Age Behavior of Bonded Concrete Overlays Due to Shrinkage and Thermal Changes, *PhD Dissertation*, University of Illinois at Urbana-Champaign, Champaign, IL, USA.
9. Janssen, D.J. (1987). Moisture in Portland Cement Concrete, *Transportation Research Record*, No. 1211, pp. 40-44.
10. Hibbitt, Karlsson and Sorensen, Inc. (1996). *ABAQUS User's Manual*, Version 5.5.
11. ACI Committee 209 (1982). *Prediction of Creep, Shrinkage, and Temperature Effects in Concrete Structures*, American Concrete Institute, p. 108, Detroit, MI, USA.
12. Bazant, Z.P. and Panula, L.P. (1982). New Model for Practical Prediction of Creep and Shrinkage, Designing for Creep and Shrinkage in Concrete Structures, *SP-76*, American Concrete Institute, pp. 7-23, Detroit, MI, USA.
13. Hansen, W. (1987). Constitutive Model for Predicting Ultimate Drying Shrinkage of Concrete, *Journal of Ceramic Society*, 70(5), pp. 329-332.
14. Lange, D. and Shin, H.C. (2001). A Computer-based Design Tool for Analysis of Bonded Concrete Overlays, *Concrete Science and Engineering*, 3(12), pp. 189-194.
15. Mindess, S., Young, J.F., and Darwin, D. (1981). *Concrete*, Prentice-Hall, Inc., Upper Saddle River, NJ, USA.
16. Kashima, S., Furuya, N., and Yamaoka, R. (1992). High-Strength Concrete for Wall Foundation Using Ternary Blended Cement with Intermixture of Blast-Furnace Slag and Fly Ash, Fly Ash, Silica Fume, Slag, & Natural Pozzolans in Concrete, *Proceedings of the 4th CANMET/ACI International Conference*, Vol. 2, pp. 1451-1469, Istanbul, Turkey.
17. Kelham, S., Damtoft, J.S., and Talling, B.L.O. (1995). The Influence of High Early-Strength (HES) Mineralized Clinker on the Strength Development of Blended Cements Containing Fly Ash, Slag, or Ground Limestone, *SP-153*, American Concrete Institute, pp. 229-248, Detroit, MI, USA.